Forced chemical mixing at Cu-Nb interfaces under severe plastic deformation

Nhon Q. Vo[a] and Robert S. Averback
Department of Materials Science and Engineering, University of Illinois, Urbana Champaign, Urbana, Illinois 61801

Yinon Ashkenazy
Department of Materials Science and Engineering, University of Illinois, Urbana Champaign, Urbana, Illinois 61801; and Racah Institute of Physics, Hebrew University of Jerusalem, Jerusalem, Israel

Pascal Bellon
Department of Materials Science and Engineering, University of Illinois, Urbana Champaign, Urbana, Illinois 61801

Jian. Wang
Los Alamos National Laboratory, Los Alamos, New Mexico 87545

(Received 23 March 2012; accepted 2 April 2012)

Forced chemical mixing during severe plastic deformation was investigated at Cu-Nb face-centered-cubic (fcc)/body-centered-cubic (bcc) interfaces using molecular-dynamics simulations. Three Cu-Nb interfaces were considered, with either Kurdjumov-Sachs or Nishiyama-Wassermann orientation relationship (OR) between fcc and bcc phases. Forced mixing of a spherical bcc-Nb precipitate in fcc-Cu was also studied for comparison. Deformation was imposed by shape-preserving cycles using two different modes, biaxial compression and biplanar shearing to investigate the effects of strain path. For biplanar shear, the chemical mixing rate is strongly dependent on structure of the interface, with the Kurdjumov-Sachs OR and a $(111)_{Cu}\|(110)_{Nb}$ habit plane being particularly resistant to mixing. During compression, no such dependence was found. Influences of interface diffuseness and roughness on stability were also investigated. The simulations show the interface mixing is inversely related to interface shear strength during shear deformation, but dominated by dislocation-glide through the Cu phase and subsequent absorption at Cu-Nb interfaces during compression deformation.

I. INTRODUCTION

Severe plastic deformation (SPD) is commonly observed to force chemical mixing and homogenization of immiscible two-phase alloys.[1–3] In systems with coherent, coexisting phases it had been suggested that such forced mixing derives from the random glide of dislocation on slip planes,[4] resulting in a mixing that is ballistic in character and independent of temperature.[5] Molecular dynamics (MD) simulations have provided quantitative support for this approximation for fcc-fcc, two-phase systems with low-to-moderate positive heats of mixing and small differences in elastic constants of the constitutive elements.[6,7] In these systems, slip can transfer across phase boundaries, which then become both rough and diffuse in response.[4,8,9]

Subsequent MD simulations by Lund et al.,[10] Vo et al.,[8] and Delogu[11] have shown that mechanical alloying in coherent alloy systems with very large positive heats of mixing or with large differences in elastic constants is not entirely ballistic, but rather it is guided by the thermochemical and mechanical properties of the alloys and it is temperature-dependent. These recent simulations are now able to explain a number of SPD experiments on coherent systems. For example, Cu-Ag alloys, which have a small positive heat of mixing, ΔH_m ($\approx$ 6 kJ/mol for the equiatomic composition), form homogeneous solid solutions during low-temperature ball milling,[12] whereas the solubility limits in Ni-Ag alloys, which have a large positive heat of mixing ($\approx$ 20 kJ/mol for the equiatomic composition), can be only slightly extended.[13] Similar results are found experimentally on alloy systems comprised of elements with different crystallographic structures. For instance, full mixing is achieved for a wide range of compositions in Cu-Fe[14–17] ($\Delta H_m \approx$ 11 kJ/mol for the equiatomic composition) and Cu-Co [Ref. 18] ($\Delta H_m \approx$ 10 kJ/mol for the equiatomic composition), but only limited extension of solubility has been achieved in Cu-Nb[19] ($\Delta H_m \approx$ 28 kJ/mol for the equiatomic composition).

Whereas forced mixing in two-phase alloys with dissimilar crystalline structures share some similarities with coherent structural systems, the detailed mechanisms of

[a]Address all correspondence to this author.
e-mail: nhonvo2@illinois.edu
DOI: 10.1557/jmr.2012.106

 © Materials Research Society 2012

https://doi.org/10.1557/jmr.2012.106 Published online by Cambridge University Press

forced mixing in these alloys remains poorly understood, and few atomistic simulations of such mixing have been performed. The complications of forced mixing in such alloys derives from the fact that mixing results from dislocation glide, and therefore available slip systems and their geometrical relationships across interfaces will directly affect both the extent and character of mixing. Interfaces between two phases, moreover, can adopt different atomic structures, even for the same orientation relationship (OR). In the present work, MD simulations are carried out on Cu-Nb (fcc/bcc) composites to study the influence of interface structures on chemical mixing forced during high strain-rate SPD. The Cu-Nb composites are chosen in this study because this system has been the subject of a number of systematic investigations that have elucidated interface structures and the interactions of dislocations with these interfaces.[20–24] In particular, interfaces, stable either mechanically or thermodynamically, have been found in recent works. For example, thermodynamically stable interfaces with the $\{111\}_{fcc} \parallel \{110\}_{bcc}$ habit plane in the Kurdjumov-Sachs (KS) or Nishiyama-Wassermann (NW) ORs can be formed by physical vapor deposition (PVD),[25] (we refer to these interfaces as {111}KS and NW, respectively) and a mechanically stable interface with the $\{112\}_{fcc} \parallel \{112\}_{bcc}$ habit plane in the Kurdjumov-Sachs (KS) OR can be formed through severe plasticity deformation via accumulative roll bonding (ARB) (referred to as {112}KS).[26,27] In the present work, we perform atomistic simulations on these three interfaces under both cyclic biaxial compression and biplanar shear deformation. In addition, we consider force mixing for the case of a spherical Nb precipitate embedded in a Cu matrix for comparison with these planar interfaces.

II. COMPUTATIONAL METHODS

The simulations were performed using Cu-Nb as the model system, represented by embedded atom method (EAM) potentials.[28] The MD code in LAMMPS[29] and visualization using OVITO[30] were employed for all simulations. Model Cu-Nb bilayers with different interfaces were constructed in the experimentally observed ORs, namely, NW, {111}KS, {112}KS, as well as a Nb particle in Cu. The planar interfaces were generated by simply joining two crystals in the ORs listed in Table I. All samples were then relaxed at 100 K for 100 ps to minimize the enthalpy. Longer time relaxations show no difference. The {111}KS interface was examined by common neighbor analysis (CNA)[31]; it showed the so-called KS1 interface structure as published previously by Demkowicz et al.[32] and Wang et al.[24] The spherical interface was constructed by placing a 5 nm diameter Nb particle in a Cu matrix with an initially random orientation. The particle rotated slightly during relaxation at 100 K for 100 ps, but it then rotated by several degrees during deformation. No clear stable OR was observed at high strains. Periodic conditions were applied in all directions for all of the simulations.

TABLE I. Orientations and dimensions of all studied interface systems.

Interface type	Orientations				Dimensions			
	Cu (FCC)		Nb (BCC)		X (nm)	Y (nm)	Layer thickness (nm)	
	x-axis	z-axis	x-axis	z-axis			Cu	Nb
Particle	$[1\bar{1}0]$	[111]	–	–	7.2	7.2	–	
{112}KS	[111]	$[11\bar{2}]$	[110]	$[11\bar{2}]$	9.4	4.9	9.7	5.1
{111}KS	$[0\bar{1}1]$	[111]	$[1\bar{1}1]$	[011]	9.7	7.1	6.0	2.2
NW	$[0\bar{1}1]$	[111]	[001]	[110]	7.9	8.5	6.6	2.5

Both biaxial compression and biplanar shear deformation were applied, using a strain rate of 5×10^9/s and a temperature of 100 K. For the sake of comparison between biaxial compression and biplanar shearing, all strain values are expressed hereafter in terms of von Mises (equivalent) strains. Biaxial compressive strains were applied cyclically by scaling atomic positions, a cycle being comprised of three steps starting with $\dot{\varepsilon}_{xx} = \dot{\varepsilon}_{yy}$, followed by $\dot{\varepsilon}_{yy} = \dot{\varepsilon}_{zz}$, and finally $\dot{\varepsilon}_{zz} = \dot{\varepsilon}_{xx}$. Each cycle produced an equivalent strain of ~0.63, with the sample returning close to its original shape. For the biplanar shear, each shear strain cycle corresponds to an equivalent strain of ~1.5. Presently, LAMMPS restricts shear deformation to the x direction on the x-z plane (ε_{xy}) and x-y plane (ε_{xz}), and the y direction on the x-y plane (ε_{yz}). Whereas this limitation of LAMMPS can be readily remedied, the asymmetry proves useful for clarifying the role of interfaces on shear mixing. We therefore first applied biplanar cyclic shears $\dot{\varepsilon}_{xy} = \dot{\varepsilon}_{xz} = \dot{\varepsilon}$, followed by $-\dot{\varepsilon}_{xz} = \dot{\varepsilon}_{yz} = \dot{\varepsilon}$, and then $-\dot{\varepsilon}_{xy} = -\dot{\varepsilon}_{yz} = \dot{\varepsilon}$, with the interface plane parallel to x-y plane. We then repeated the deformation, but with the interface parallel to the x-z plane and then parallel to the y-z plane. We focus on the biplanar shearing for the Cu/Nb interface parallel to the x-y plane, as this orientation reveals more directly the effect of interface shear strength on chemical mixing, but we provide results for the other interface planes as well. We define the interface shear strength (ISS) as the flow stress in the shearing direction.

III. RESULTS AND DISCUSSIONS

A. Evolution and mixing of initially sharp interfaces

We first consider atomically sharp interfaces, beginning the analysis using the chemical short-range order parameter, Ω, as defined by Lund and Schuh[10]:

$$\Omega = \frac{\frac{c}{1-c}N_A^B + \frac{1-c}{c}N_B^A}{N_A^A + N_B^B} - 1 \quad . \qquad (1)$$

https://doi.org/10.1557/jmr.2012.106 Published online by Cambridge University Press

Here N_A^B is the average number of B-nearest neighbors around A-atoms and c is the atomic fraction of A in the A-B alloy. Ω has values of −1, 0 or 1 for microstructures that are fully decomposed (i.e., phase-separated), random, or fully ordered, respectively; Ω is essentially a measure of A-B bonds, in this case Cu-Nb bonds. Short-range order and the number of Cu-Nb bonds for the particle interface under cyclic compression are plotted in Fig. 1(a) as a function of strain. After a strain of $\varepsilon_{eq} = 110$, the system does not reach steady state, but it does show a significant amount of chemical mixing. Figures 1(b)–1(d) show the atomic configurations at equivalent strains of 0, 28, and 112, respectively, confirming the increase in disorder as a function of strain. A noteworthy feature in these figures is the amorphization of Cu regions surrounding the Nb particles; these regions are enriched with Nb atoms. The centrosymmetry parameter[33] was used to confirm the formation of an amorphous structure. Similar behavior was reported recently for spherical Nb particles in Cu, where it was shown that the amorphous Cu-Nb structure is metastable under SPD.[7] The observation of an amorphous interface structure helps to explain our finding noted above that the Nb particle does not find a steady state orientation in Cu during shearing; the amorphous layer removes any significant anisotropy in the Cu-Nb OR. These simulations also reveal that the mixing is highly asymmetric, with Nb atoms broadly distributed throughout the Cu matrix, but virtually no Cu atoms within the Nb particle. We discuss this asymmetry in more detail, below.

Chemical mixing (i.e., number of Cu-Nb bonds) in systems under biaxial compression and biplanar shear deformation are plotted as a function of strain in Figs. 2(a) and 2(b), respectively. Under compression, chemical mixing rates are essentially identical for the three interfaces investigated, and they are also equal to that for the Nb particle. For shear, in contrast, the behavior is quite different. Chemical mixing for the {112}KS interface under shear is far more efficient than for the NW and {111}KS interfaces, and approximately equal to that for the Nb particle. Notably, chemical mixing of {111}KS interface is nearly absent at strains as high as 150. The NW interface is stable up to a strain of 30, but then the mixing rate begins to increase rapidly. Atomic configurations of the four interfaces after an equivalent strain of 100 under shear are shown in Fig. 3, illustrating the strong effect of the interface structure on atomic mixing under biplanar shear. We remind the reader that these results for biplanar shear pertain to Cu/Nb interface lying in the x-y plane of the simulation cell and that there are no shearing forces in the direction normal to the interface plane for this geometry.

Concentration profiles across the {112}KS interface as a function of strain are plotted in Figs. 4(a) and 4(b) for both deformation modes. It can be observed that the {112}KS interface becomes diffuse faster under compression compared to shearing, in agreement with the results shown

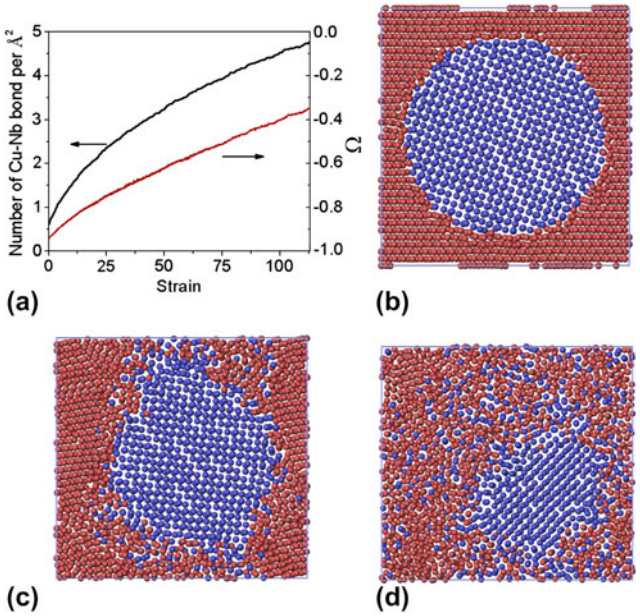


FIG. 1. (a) Short-range order and number of Cu-Nb bonds per unit initial interfacial area as a function of strain of Cu-Nb particle interface. Cross sectional slice through the center of the computational cell at strain of 0 (b), 28 (c), and 112 (d) (Cu: red, Nb: blue).

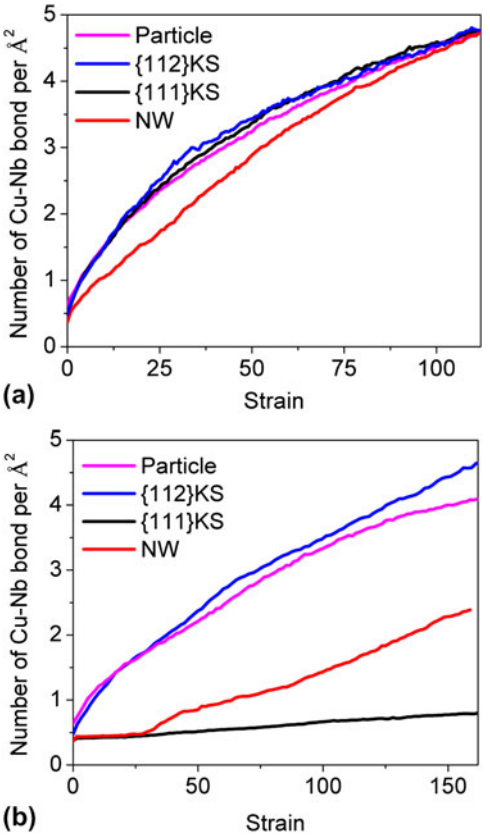


FIG. 2. Strain evolution of chemical mixing in different interfaces under (a) biaxial compression deformation, and (b) biplanar shear deformation.

https://doi.org/10.1557/jmr.2012.106 Published online by Cambridge University Press

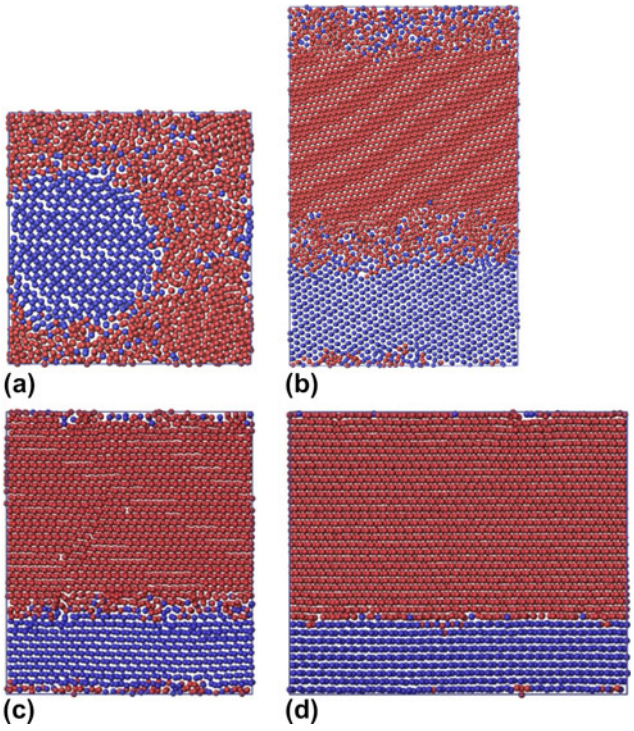


FIG. 3. Atomic configuration at strain of 100 of (a) particle (b) {112} KS (c) NW and (d) {111}KS interface under biplanar shear deformation (Cu: red, Nb: blue).

in Fig. 2. After an equivalent strain of 10, which is a typical strain level in ARB and wire drawing processes,[34] a diffuse interface has formed, with its width ranging from 1 to 2 nm in both deformation modes. Concentration profiles across the various interfaces after a strain of 20 under compression and 100 under shear deformation are plotted in Figs. 4(c) and 4(d), respectively. In compression, there are no significant differences in the chemical mixing profiles at the different interfaces. A large difference is observed, however, under shear, again confirming the difference in mixing rates shown in Fig. 2(b).

Another key feature revealed in Fig. 4 concerns the shape of the concentration profiles during mixing. At strains of 10, under compression, the concentration profiles are symmetric and the widths of the interfaces are ≈ 1–2 nm [Fig. 4(a)]. At higher strains, the concentration profiles for all interfaces become asymmetric with a long Nb tail extending into the Cu phase. This is consistent with the fact that Nb atoms once transported away from the interface undergo very rapid mixing in the Cu phase, owing to the unobstructed glide of dislocations in that phase.[6] In contrast, Cu atoms that have been transported in the Nb phase have very limited mobility since there is only little dislocation activity in the Nb phase. This results in strongly asymmetric composition profiles. A similar asymmetry is observed during biplanar shear deformation of the {112}KS interface. For the {111}KS interface, the interface remains very narrow under biplanar shear, even at strains up to 150. The contribution of the very fast transport of Nb atoms in the Cu phase, therefore, is minimal, and the composition profile remains symmetric. We conclude this section by pointing out that the experimental observation of asymmetric composition profiles in dissimilar materials forced by SPD[35] is perfectly compatible with dislocation-based mixing mechanisms, without any contribution from thermal diffusion.

As discussed in the introduction, atomistic simulations indicate that chemical mixing in immiscible systems is driven by dislocation glide.[6,7] We therefore tracked the dislocation activity in both deformation modes. This was accomplished by measuring the relative motion of pairs of atoms with Cu-Cu bonds (bulk Cu), Nb-Nb bonds (bulk Nb), and Cu-Nb bonds (interface) during initial straining (see Ref. 6 for details). The mean square relative displacement (MSRD) between nearest neighbor pairs of atoms, $\sigma^2_{XY}(t_1, t_2)$, is given by,

$$\sigma^2_{XY}(t_1,t_2) = \frac{\sum_{i=1}^{N_X}\sum_{j=1}^{Z_Y(i)}\left[(R_{ij})_{t_2} - (R_{ij})_{t1}\right]^2}{6(1+\delta_{XY})\sum_{i=1}^{N_X} Z_Y(i)} \quad , \qquad (2)$$

where, $(R_{i,j})_{t1}$ is the vector connecting an atom i to a nearest neighbor atom j at time t_1; $(R_{i,j})_{t2}$ is that vector at a later time t_2; N_X is the number of atoms of type X, z_Y is the number of nearest neighbor XY pairs, and $\delta_{XY} = 1$ if X = Y, and 0 otherwise. In the following, MSRDs are measured over a time interval t_2-t_1 corresponding to one deformation cycle. σ^2_{CuCu} and σ^2_{NbNb} provide a measure for the amount of shear mixing in bulk Cu and Nb respectively, and they are related to the plastic strain in those phases.[6] Figure 5, for example, shows the deformation due to glide of partial dislocations, resulting in stacking faults and perfect dislocations. σ^2_{CuNb} similarly provides a measure of the amount of shearing and mixing that occurred at Cu-Nb interface, resulting from either dislocations crossing through the interface, interface shearing (Cu and Nb crystals sliding on each other), or atomic rearrangements in the interface where dislocations are absorbed, i.e., atomic shuffling. If σ^2_{CuNb} results from dislocations crossing the interface, it should be correlated to σ^2_{CuCu} and σ^2_{NbNb}. On the other hand, if σ^2_{CuNb} results from interface shearing, it should be independent of σ^2_{CuCu} and σ^2_{NbNb}, and if it is due to atomic shuffling, it should be proportional to the larger value out of σ^2_{CuCu} and σ^2_{NbNb}.

MSRD for all pairs at small strain, evaluated between strains of 0 and 15 are shown in Figs. 6(a) and 6(b) for compression and shear, respectively. Under compression, σ^2_{CuCu} is much larger than σ^2_{NbNb}, by a factor ≈ 8 for the particle, {112}KS, and NW interfaces, and by a factor ≈ 2 for the {111}KS interface. The MSRD value for Cu-Nb

https://doi.org/10.1557/jmr.2012.106 Published online by Cambridge University Press

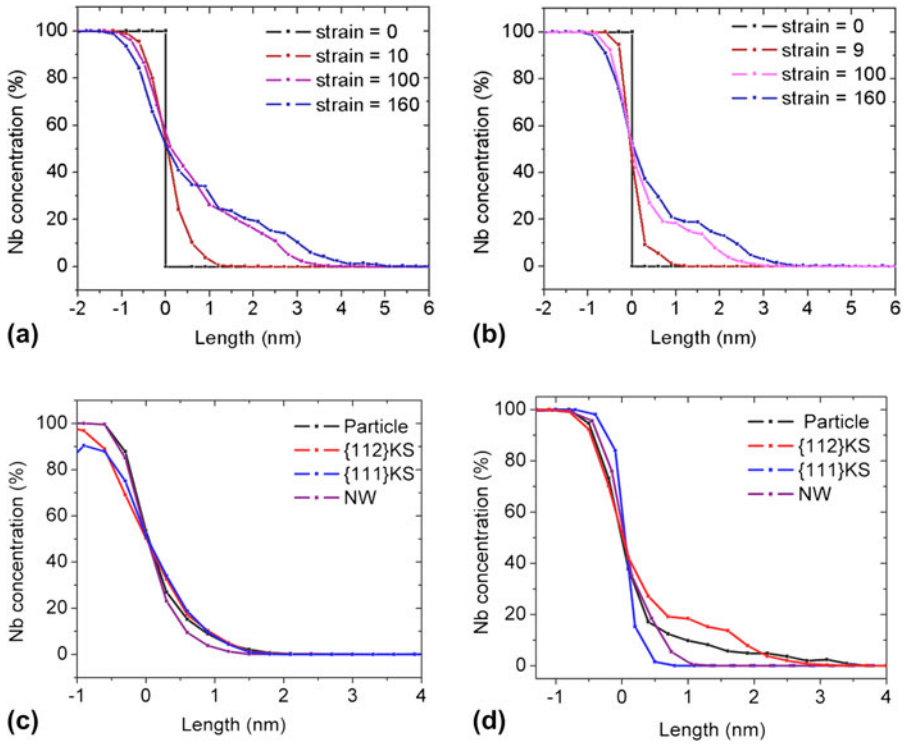


FIG. 4. Concentration profile through {112}KS interface as a function of strain under (a) biaxial compression and (b) biplanar shear. Concentration profile through all studied interface systems (c) at strain of 20 under biaxial compression and (d) at strain of 100 under biplanar shear. Atomic configurations are shown in Fig. 3.

interface pairs, moreover, is similar to bulk Cu for all interfaces. Figure 6(a) thus suggests that plasticity in all studied interface systems under compressive deformation behave similarly. Plastic deformation is localized in the Cu phase, which is not surprising because nucleation and glide of dislocations in Cu is easier than in Nb.[2,6,11] We surmise, therefore, that dislocations are mainly confined to the Cu lattice, but when they are absorbed in the Cu-Nb interface, they give rise to atomic shuffling, accompanied by interface reconstruction and/or a reduction in the local density of dislocations within the interfaces. Such shuffling reactions were recently discussed as a deformation mechanism in pure nanocrystalline metals.[36] Thus, forced mixing results from dislocations impinging on an interface, but in contrast to systems with coherent interfaces,[4,6] the mixing is not due to dislocations crossing interfaces, but to their emission and absorption at interfaces. The mixing rate in compression is observed to be independent of the interface orientation. This can be understood by considering dislocation nucleation. In uniaxial tension, Zhang et al.[23] showed that the stress state promotes dislocation loop nucleation from the network of interface dislocations for all interfaces investigated here. Once nucleated, the segments of these dislocation loops lying in the Cu phase expand (as illustrated in Fig. 5), rather than shearing the interface. Therefore, the chemical mixing rate is expected to be largely insensitive to the details of the interface, as we observe here.

Under shear deformation, Fig. 6(b), a large difference in MSRD values for different interfaces is observed. First, as for compressive strain, localization of plastic deformation is observed in the Cu phase. For the embedded Nb particle, the MSRD values in bulk Cu and the Cu-Nb interface are similar and about $\approx$ 100 times larger than in bulk Nb. MSRD values for the {111}KS and NW interfaces, on the other hand, are much higher for Cu-Nb pairs and lower values for Cu-Cu pairs in comparison to those for the particle and the {112}KS interface. This illustrates that many shearing events occur within interface planes of {111}KS and NW interfaces rather than in bulk Cu. Visualization (not shown) confirms that the high value of MSRD of Cu-Nb pairs derives from interface shearing rather than dislocations crossing the interface. This observation thus provides the explanation for the large difference in chemical mixing rate under biplanar shear versus biaxial compression. Recall that in the systems studied so far, the interface is parallel to the *x*-*y* plane, and therefore four out of the six shear deformations imposed in each biplanar shear cycle are applied parallel to the interface plane. When such shearing is localized at the interface plane (Cu and Nb phase sliding on each other), chemical mixing is dramatically reduced because few atoms are

https://doi.org/10.1557/jmr.2012.106 Published online by Cambridge University Press

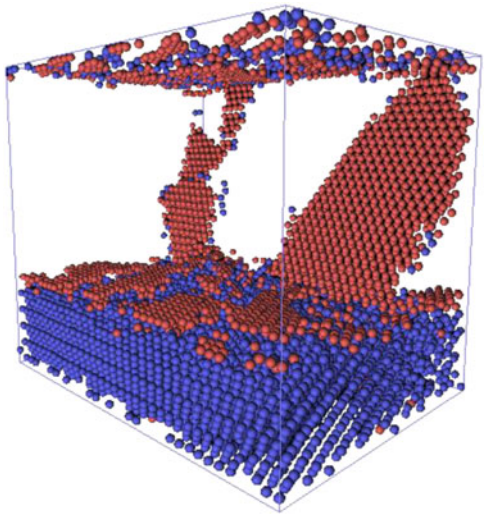


FIG. 5. Snapshot of the configuration of a {111}KS interface sample during straining. Blue atoms are Nb, red atoms are stacking faults (bounded by partial dislocations) in Cu, the rest of Cu atoms are not shown.

forced across the interface. These results are in agreement with recent findings by Wang et al.[24] that the interface shear strengths of Cu-Nb {111}KS and NW interfaces are particularly low, the lowest value being 400 MPa for {111}KS and 250 MPa for NW.[22,23] The {112}KS interface, moreover, has the highest flow stress and it is highly anisotropic, the lowest value being 1000 MPa along the $[0\bar{1}1]_{Cu} \parallel [1\bar{1}1]_{Nb}$ direction.[37]

B. Evolution and mixing of initially diffuse interfaces

For better understanding the relationship between the chemical stability of {111}KS interface and interface shear strength we varied the ISS of {111}KS interfaces by replacing the sharp interface by one that is slightly diffuse. This was accomplished by randomly switching Cu and Nb atoms located within three layers of the interface, creating a symmetric profile with the first, second, and third layers having compositions X, X/2, and X/4, with X ranging from 0 to 25 at.%, as illustrated in Fig. 7. Interface shear strength was then measured as a function of the initial diffuseness X of {111}KS interfaces in the x and y directions; these correspond to $[1\bar{1}0]$ and $[11\bar{2}]$ in the Cu crystal [Fig. 8(a)]. For a sharp {111}KS interface, X = 0 at.%, $\tau_{[1\bar{1}0]}$ and $\tau_{[11\bar{2}]}$ are found to be ≈ 0.35 and ≈ 0.62 GPa respectively, illustrating the anisotropic behavior of ISS, as reported in ref. [24]. As the level of diffuseness increases, ISS is observed to increase in both directions as seen in Fig. 8(a). At X = 15 at.%, ISS starts to saturate, and beyond X = 15 at.%, values of $\tau_{[1\bar{1}0]}$ and $\tau_{[11\bar{2}]}$ become similar, 0.8–0.9 GPa, indicating a more isotropic ISS. This result can be understood in terms of the corresponding interface structures, as illustrated in

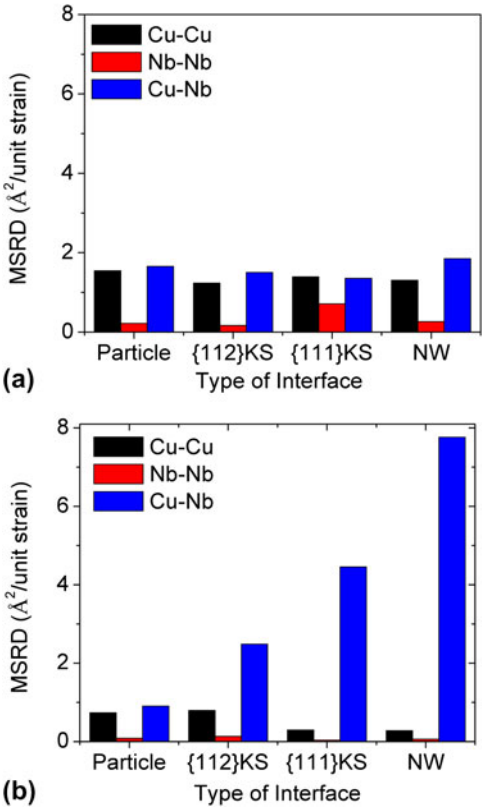


FIG. 6. Mean square relative displacements of atomic pairs, per unit strain, for different interface types under (a) biaxial compression deformation and (b) biplanar shear deformation.

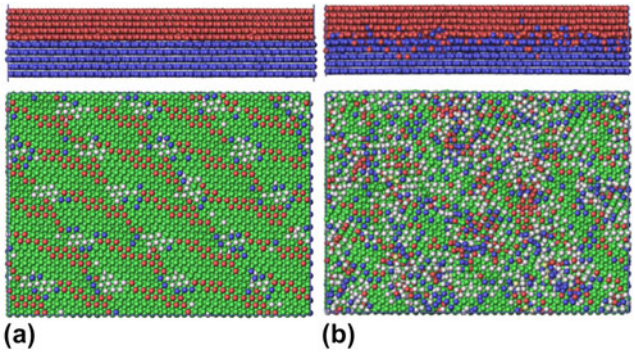


FIG. 7. (a) Cross-section (top) and interface plane-view (bottom) of {111}KS interface. CNA was performed on first plane of Cu showing two sets of misfit interface dislocations. Colors are based on local symmetry from CNA: green for fcc, red for hcp, blue for bcc, white otherwise. (b) Cross-section and interface plane-view of {111}KS diffuse interface for X = 15 at.%. CNA was performed on first plane of Cu showing a more disordered interface compared with a {111}KS interface.

Figs. 7(a) and 7(b) for X = 0 at.% and 15 at.%, respectively. As diffuseness increases, the interface structure transforms from an ordered array of misfit dislocations[32] to an amorphous structure, and thus it is anticipated that interface

https://doi.org/10.1557/jmr.2012.106 Published online by Cambridge University Press

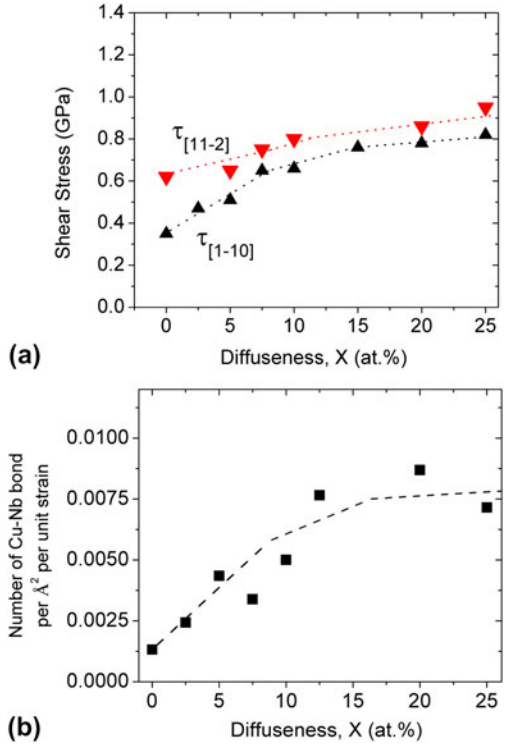


FIG. 8. (a) Interface shear strength of both x and y orientations as a function of diffuseness of {111}KS interface. (b) Chemical mixing rate as a function of diffuseness X of {111}KS interface under biplanar shear deformation.

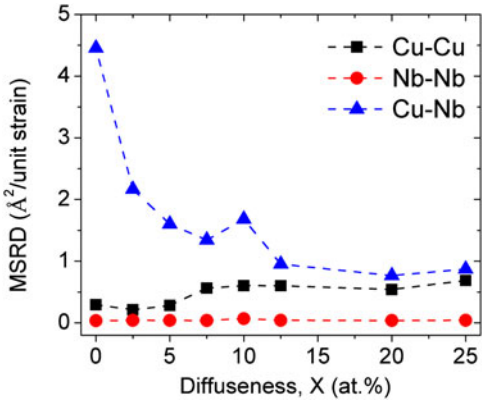


FIG. 9. Mean square relative displacement of atomic pairs, per unit strain, as a function of diffuseness X of {111}KS interface under biplanar shear deformation mode.

properties such as ISS will evolve from highly anisotropic to isotropic.

The initial chemical mixing rate, measured from strain of 0–15, is observed to depend strongly on the diffuseness of the {111}KS interface under biplanar shear deformation, as seen in Fig. 8(b). As the diffuseness increases, the chemical mixing rate also increases significantly, saturating at X ≈ 15 at.%. The trend is therefore that a sharp {111}KS interface has low ISS and high chemical stability under shear, whereas the opposite is true for a highly diffuse {111}KS interface. We also find this correlation between ISS and the MSRD of nearest neighbor Cu-Cu, Nb-Nb and Cu-Nb pairs, as shown in Fig. 9. Whereas deformation appears to be confined to interface shearing for sharp {111}KS interfaces, the Cu-Cu and Cu-Nb pair diffusion coefficients converge toward similar values as the diffuseness exceeds 12.5 at.%, thus suggesting that the dominant plastic deformation mode has changed from interface shearing to bulk deformation of the Cu phase. Mixing is then enhanced by dislocations gliding into the interface and stimulating atomic shuffling.

Quantitative analysis of mixing indicates that at a diffuse {111}KS interface with X = 25 at.% the rate of creation of Cu-Nb bonds per Å^2 is $\approx 7.1 \times 10^{-3}$, which approaches the initial rate measured for the particle case and for the {112}KS interface, $\approx 2.0 \times 10^{-2}$, see Fig. 2(b).

A diffuse {111}KS is therefore no more resistant to forced chemical mixing than are general interfaces. The present results also indicate that there should be a positive feedback loop between strain and mixing rate even at a sharp {111}KS interface. As strain increases, the diffuseness of the interface slowly increases, which in turn raises the resistance to interface shearing—the interface becomes "stronger" with strain, thus promoting dislocation activity at and near the interface, which ultimately will increase the mixing rate. A slight increase of the slope of chemical mixing is indeed measured for the sharp {111}KS interface, as shown in Fig. 2(b), but simulations to even larger strains would be necessary to confirm this prediction. The response of the NW interface, see Fig. 2(b), suggests also that a transition from low to high mixing rates can take place in a nearly "catastrophic" manner, akin to a bifurcation.

C. Evolution and mixing of stepped interfaces

We also explored the effect of interface roughness on ISS and shear mixing by creating single-layer step edges. This was done by first joining Cu and Nb crystals in KS OR with one layer of (111) Cu and (110) Nb overlapping. Part of the Cu and Nb overlapped layer was then cut out to create a pair of steps on the interface [see Figs. 10(a) and 10(b)]. Similar procedures were used to create a different number of pairs of steps. These pairs of steps have the same width and are equally spaced. The steps were created along both x (Cu[110]) and y (Cu[112]) directions. Up to five pairs of steps along the x direction and seven pairs of steps along the y direction were created. All the created samples were relaxed at 100 K for 100 ps to minimize their energy. The results are shown in Fig. 11(a) (step edge along y-axis) and Fig. 11(b) (step edge along x-axis). Samples with steps behave similarly, independent of the direction of the steps. Initially, larger number of steps results in higher chemical mixing rate. All chemical

https://doi.org/10.1557/jmr.2012.106 Published online by Cambridge University Press

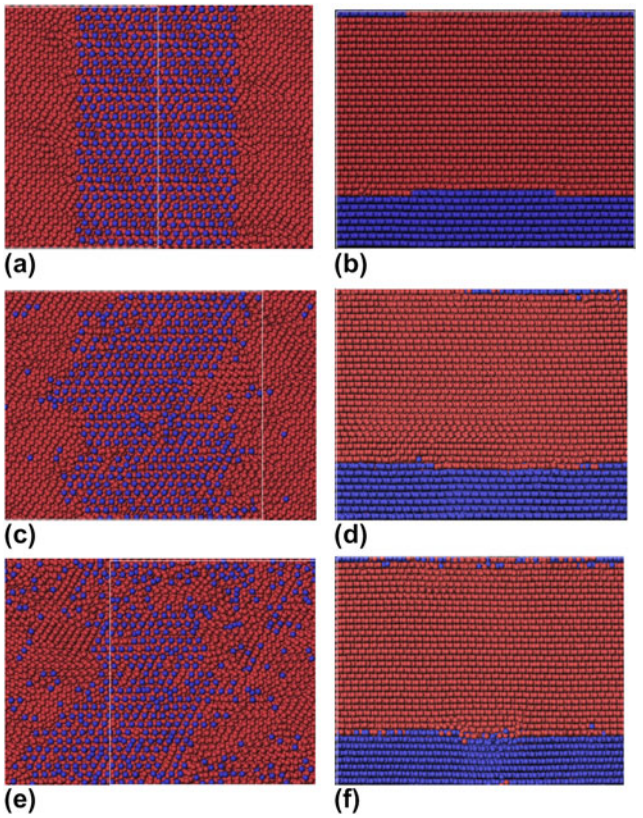


FIG. 10. Interface plane-view (a,c,e) and cross-section (b,d,f) of 2-step {111}KS interface at strain of 0 (a,b), 15 (c,d), 59 (e,f). Cu: red, Nb: blue.

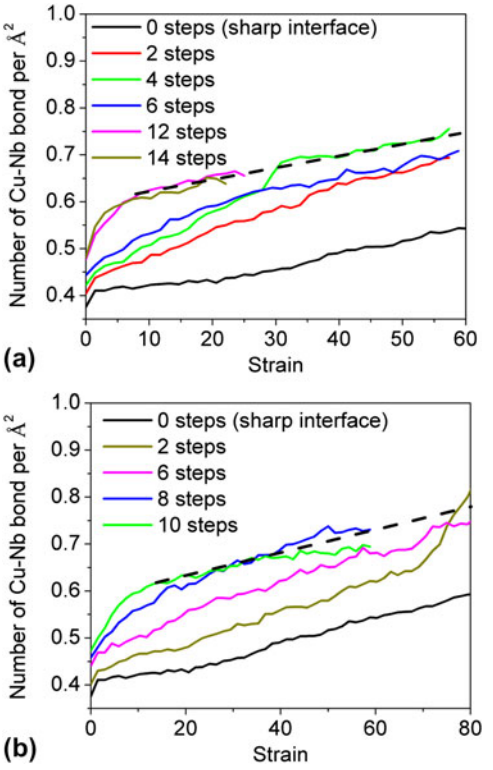


FIG. 11. Strain evolution of chemical mixing for different step numbers along (a) y direction (Cu[112]) and (b) x direction (Cu[110]) for {111}KS interface.

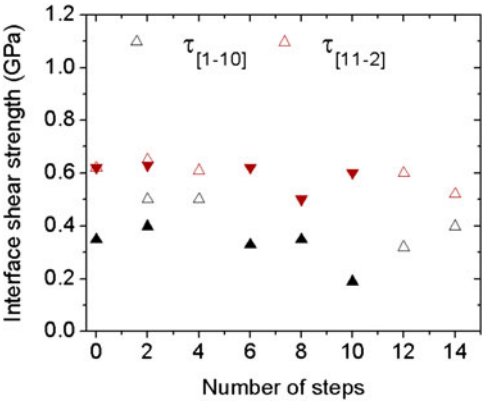


FIG. 12. Interface shear strength of two orientations as a function of number of steps in $[11\bar{2}]$ (open symbols) and $[1\bar{1}0]$ (solid symbols) directions for {111}KS interface.

mixing curves however, come to the same steady state rate of mixing after a brief period of relaxation (strain), which is equal to the mixing rate for the sharp and planar {111} KS interface. We also note that the same steady state is observed for both step directions. Figures 10(a)–10(f) show plane and cross-sectional views of the interface at different strains in a sample initially containing one pair of steps. Figures 10(a), 10(c), and 10(e) show that Nb atoms initially belonging to the step layer become randomly distributed throughout the layer as strain increases. Figures 10(b), 10(d), and 10(f), indicate, however, that Nb relocation occurs only on the step layer (z plane), and not below the interface plane, even at a strain of 59. Similar behavior was observed when multiple steps were introduced. Since Nb atoms are randomly distributed on the step layer in all cases, all interfaces reach similar configurations, and therefore should also reach similar mixing rates at steady state, and this is indeed observed in Figs. 11(a) and 11(b). ISS of all studied step interfaces along x and y directions are plotted in Fig. 12. For all cases, there is no significant effect of steps on the ISS, or on its anisotropy. We thus conclude that the presence of *single-layer steps* is not sufficient to prevent interface sliding since it did not affect the interface shear strength. Since it has been observed that larger steps present nucleation sites for dislocation,[23,38] it is reasonable to expect that larger steps will decrease the chemical stability of {111}KS interface to shear deformation, but we have not examined this possibility in this work.

D. Effect of interface orientation during biplanar shearing of KS interfaces

Finally, we investigate the effect of the interface orientation on the stability of {111}KS and {112}KS

https://doi.org/10.1557/jmr.2012.106 Published online by Cambridge University Press

interfaces during biplanar shearing. The results presented so far were for the interface parallel to the *x-y* plane; we now consider cases for it parallel to the *y-z* and *z-x* planes. Note that when the interface plane is parallel to the *z-x* plane, two out of the six steps in the cycle contain shear forces normal to the interface plane, and when the interface is parallel to the *y-z* plane, four steps in the cycle contain shear forces normal to the interface plane. As shown in Fig. 13(a), the mixing at {111}KS interfaces increases substantially as the interface plane is switched from the *x-y* plane to the *z-x* plane, and then again as it is switched to the *y-z* plane. We conclude therefore that in the case of low ISS interfaces, such as {111}KS, there exists a direct correlation between shear mixing and the number of steps in the biplanar shear cycle that have force components normal to the interface plane: Efficient shear mixing of the {111}KS interface requires shear forces normal to its habit plane. No effect, on the other hand, is observed for the {112}KS interface, which is expected owing to the high shear strength of that interface, especially in the $<111>_{Cu} \parallel <110>_{Nb}$ direction. *We emphasize, however, that for all three interface orientations the {111}KS interfaces are more resistant to mixing than {112}KS interfaces, as shown in* Fig. 13(a). Part of this high resistance of {111}KS interfaces to mixing originates from easy interface sliding when shear forces are applied in the interface plane. This factor alone is however not sufficient to rationalize our results as {111}KS mixing is also low for interfaces in the *y-z* plane, that is so, even when shear forces are applied perpendicular to the interface plane. Visualization of atomic configurations shows that, in that case, dislocations gliding through the layers can be absorbed by the {111}KS interface, in agreement with the attractive interactions between lattice dislocations and KS interfaces reported by Wang and Misra.[39] Once stored at the interface, dislocations can later react and annihilate with other stored dislocations, or can be re-emitted during a subsequent step of the strain cycle. The mixing rate for {111}KS interfaces parallel to *y-z* plane is measured to increase with the strain per cycle, as illustrated in Fig. 13(b). This increase is consistent with the fact that dislocation storing at interfaces is more effective when the dislocation density is low. We conclude this section by noting that the higher overall resistance to forced mixing of {111}KS interfaces over {112}KS interfaces reported here suggests that it would be interesting to measure experimental mixing rates for Cu/Nb multilayers obtained by PVD and by ARB, since the dominant interfaces in these materials are {111}KS and {112}KS, respectively.

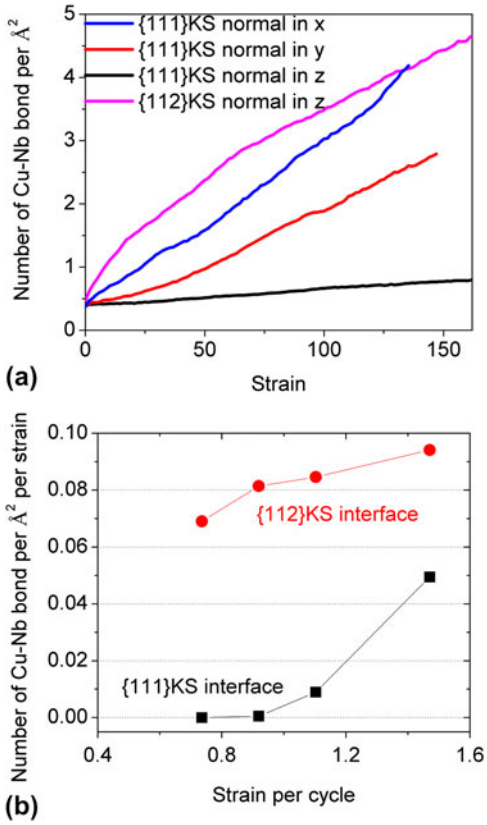


FIG. 13. (a) Chemical mixing evolution of KS interface, where interface normal is on different axis. {112}KS interface is included for reference. (b) Initial chemical mixing rate as a function of strain/cyle of {111}KS and {112}KS interface.

IV. CONCLUSION

The forced chemical mixing of atoms in different Cu-Nb fcc/bcc interface systems during SPD has been investigated using MD computer simulations. Under biaxial compression deformation, the chemical mixing rate is independent of interface type. However, under biplanar shearing deformation, the chemical mixing rate is strongly dependent on interface type, and the {111}KS interface shows remarkable chemical stability at equivalent strains exceeding 150, whereas NW interfaces remain stable up to equivalent strains of 30. In this deformation mode, analysis shows that interface shear strength and interface chemical stability are directly related. The easier it is to shear an interface, the more stable it is under shear. Diffuse {111}KS interfaces have a higher interface shear strength compared to a sharp {111}KS interface, thus leading to a progressive loss of chemical stability of these interfaces as the diffuseness increases. In contrast, it is shown that single-layer step {111}KS interfaces have the same ISS as the perfectly planar {111}KS interface. Therefore, these steps are not expected to modify the chemical stability of specific interfaces during deformation, which is indeed what was observed in the simulations. The present work offers a clear guide for the design of Cu-Nb interfaces with high chemical stability during shear deformation.

https://doi.org/10.1557/jmr.2012.106 Published online by Cambridge University Press

ACKNOWLEDGMENTS

This research was supported as part of the Center for Materials at Irradiation and Mechanical Extremes, an Energy Frontier Research Center funded by the U.S. Department of Energy, Office of Science, Basic Energy Sciences, under Award No. 2008LANL1026. Additional support (for N.Q. Vo) was provided by the U.S. Department of Energy, Office of Science, Basic Energy Sciences under Grant DEFG02-05ER46217.

REFERENCES

1. G. Martin and P. Bellon: Driven alloys. *Solid State Phys.* **50**, 189 (1997).
2. C. Suryanarayana: Mechanical alloying and milling. *Prog. Mater Sci.* **46**, 1 (2001).
3. E. Ma: Alloys created between immiscible elements. *Prog. Mater Sci.* **50**, 413 (2005).
4. P. Bellon and R.S. Averback: Nonequilibrium roughening of interfaces in crystals under shear—application to ball-milling. *Phys. Rev. Lett.* **74**, 1819 (1995).
5. G. Martin: Phase-stability under irradiation—ballistic effects. *Phys. Rev. B* **30**, 1424 (1984).
6. S. Odunuga, Y. Li, P. Krasnochtchekov, P. Bellon, and R.S. Averback: Forced chemical mixing in alloys driven by plastic deformation. *Phys. Rev. Lett.* **95**, 045901 (2005).
7. Y. Ashkenazy, N.Q. Vo, D. Schwen, R.S. Averback, and P. Bellon: Shear induced chemical mixing in heterogeneous systems. *Acta Mater.* **60**, 984 (2012).
8. N.Q. Vo, S. Odunuga, P. Bellon, and R.S. Averback: Forced chemical mixing in immiscible alloys during severe plastic deformation at elevated temperatures. *Acta Mater.* **57**, 3012 (2009).
9. D. Schwen, R.S. Averback, and P. Bellon (in preparation).
10. A.C. Lund and C.A. Schuh: Driven alloys in the athermal limit. *Phys. Rev. Lett.* **91**, 235505 (2003).
11. F. Delogu: Forced chemical mixing in model immiscible systems under plastic deformation. *J. Appl. Phys.* **104**, 073533 (2008).
12. T. Klassen, U. Herr, and R.S. Averback: Ball milling of systems with positive heat of mixing: Effect of temperature in Ag-Cu. *Acta Mater.* **45**, 2921 (1997).
13. J. Xu, U. Herr, T. Klassen, and R.S. Averback: Formation of supersaturated solid solutions in the immiscible Ni-Ag system by mechanical alloying. *J. Appl. Phys.* **79**, 3935 (1996).
14. J. Eckert, J.C. Holzer, C.E. Krill, and W.L. Johnson: Mechanically driven alloying and grain-size changes in nanocrystalline Fe-Cu powders. *J. Appl. Phys.* **73**, 2794 (1993).
15. J.Y. Huang, Y.D. Yu, Y.K. Wu, D.X. Li, and H.Q. Ye: Microstructure and nanoscale composition analysis of the mechanical alloying of Fe_xCu_{100-x} (X = 16, 60). *Acta Mater.* **45**, 113 (1997).
16. E. Ma, M. Atzmon, and F.E. Pinkerton: Thermodynamic and magnetic properties of metastable Fe_xCu_{100-x} solid-solutions formed by mechanical alloying. *J. Appl. Phys.* **74**, 955 (1993).
17. E. Ma, J.H. He, and P.J. Schilling: Mechanical alloying of immiscible elements: Ag-Fe contrasted with Cu-Fe. *Phys. Rev. B* **55**, 5542 (1997).
18. C. Gente, M. Oehring, and R. Bormann: Formation of thermodynamically unstable solid solutions in the Cu-Co system by mechanical alloying. *Phys. Rev. B* **48**, 13244 (1993).
19. E. Botcharova, J. Freudenberger, and L. Schultz: Mechanical and electrical properties of mechanically alloyed nanocrystalline Cu-Nb alloys. *Acta Mater.* **54**, 3333 (2006).
20. M.J. Demkowicz, J. Wang, and R.G. Hoagland: Interfaces between dissimilar crystalline solids, in *Dislocations in Solids*, Vol. 14, Chap. 83, edited by J.P. Hirth (Elsevier, Amsterdam, Netherlands, 2008), pp. 141–207.
21. W.Z. Han, J.S. Carpenter, J. Wang, I.J. Beyerlein, and N.A. Mara: Atomic-level study of twin nucleation from face-centered-cubic/body-centered-cubic interfaces in nanolamellar composites. *Appl. Phys. Lett.* **100**, 011911 (2012).
22. J. Wang, R.G. Hoagland, X.Y. Liu, and A. Misra: The influence of interface shear strength on the glide dislocation-interface interactions. *Acta Mater.* **59**, 3164 (2011).
23. R.F. Zhang, J. Wang, I.J. Beyerlein, and T.C. Germann: Dislocation nucleation mechanisms from fcc/bcc incoherent interfaces. *Scr. Mater.* **65**, 1022 (2011).
24. J. Wang, R.G. Hoagland, J.P. Hirth, and A. Misra: Atomistic simulations of the shear strength and sliding mechanisms of copper-niobium interfaces. *Acta Mater.* **56**, 3109 (2008).
25. K. Yu-Zhang, J.D. Embury, K. Han, and A. Misra: Transmission election microscopy investigation of the atomic structure of interfaces in nanoscale Cu-Nb multilayers. *Philos. Mag.* **88**, 2559 (2008).
26. S.C.V Lim and A.D. Rollett: Length scale effects on recrystallization and texture evolution in Cu layers of a roll-boned Cu-Nb composite. *Mater. Sci. Eng., A* **520**, 189 (2009).
27. J.S. Carpenter, S.C. Vogel, J.E. vLeDonne, D.L. Hammon, I.J. Beyerlein, and N.A. Mara: Bulk texture evolution of Cu/Nb nanolamellar composites during accumulative roll bonding. *Acta Mater.* **60**, 1576 (2012).
28. M.J. Demkowicz and R.G. Hoagland: Structure of Kurdjumov-Sachs interfaces in simulations of a copper-niobium bilayer. *J. Nucl. Mater.* **372**, 45 (2008).
29. S. Plimpton: Fast parallel algorithms for short-range molecular-dynamics. *J. Comput. Phys.* **117**, 1 (1995).
30. A. Stukowski: Visualization and analysis of atomistic simulation data with OVITO—the open visualization tool. *Mater. Sci. Eng.* **18**, 015012 (2010).
31. D. Faken and H. Jonsson: Systematic analysis of local atomic structure combined with 3D computer graphics. *Comput. Mater. Sci.* **2**, 279 (1994).
32. M.J. Demkowicz, R.G. Hoagland, and J.P. Hirth: Interface structure and radiation damage resistance in Cu-Nb multilayer nanocomposites. *Phys. Rev. Lett.* **100**, 136102 (2008).
33. C.L. Kelchner, S.J. Plimpton, and J.C. Hamilton: Dislocation nucleation and defect structure during surface indentation. *Phys. Rev. B* **58**, 11085 (1998).
34. R.Z. Valiev, R.K. Islamgaliev, and I.V. Alexandrov: Bulk nanostructured materials from severe plastic deformation. *Prog. Mater. Sci.* **45**, 103 (2000).
35. X. Quelennec, A. Menand, J.M. Le Breton, R. Pippan, and X. Sauvage: Homogeneous Cu-Fe supersaturated solid solutions prepared by severe plastic deformation. *Philos. Mag.* **90**, 1179 (2010).
36. H.V. Swygenhoven and P.M. Derlet: Grain-boundary sliding in nanocrystalline fcc metals. *Phys. Rev. B* **64**, 224105 (2001).
37. M.J. Demkowicz and L. Thilly: Structure, shear resistance and interaction with point defects of interfaces in Cu-Nb nanocomposites synthesized by severe plastic deformation. *Acta Mater.* **59**, 7744 (2011).
38. J.A. Brown and N.M. Ghoniem: Structure and motion of junctions between coherent and incoherent twin boundaries in copper. *Acta Mater.* **57**, 4454 (2009).
39. J. Wang and A. Misra: An overview of interface-dominated deformation mechanisms in metallic multilayers. *Curr. Opin. Solid State Mater. Sky.* **15**, 20 (2011).

https://doi.org/10.1557/jmr.2012.106 Published online by Cambridge University Press